Published in EPL (Europhysics Letters) 41, issue 2, 141-146, 1998
which should be used for any reference to this work

A continuous beam of slow, cold cesium atoms magnetically extracted from a 2D magneto-optical trap

P. Berthoud, A. Joyet, G. Dudle(*), N. Sagna(**) and P. Thomann

Observatoire Cantonal - Rue de l'Observatoire 58, CH-2000 Neuchâtel, Switzerland

Abstract. – Starting from a 2D magneto-optical trap where cesium atoms are permanently subjected to 3D sub-Doppler cooling and 2D magneto-optical trapping, we have produced a beam of cold atoms continuously extracted along the trap axis. The simplest extraction mechanism, presently used, is the drift velocity induced by a constant magnetic field. We have used this continuous beam of atoms to produce Ramsey fringes in a microwave cavity as a first demonstration of an atomic resonator operating continuously with laser cooled atoms. The shape of the resonance pattern allows an estimate of the axial temperature, typically 200 μK. The average velocity can be adjusted from 0.7 to 3 m/s; the *trap-to-atomic-beam* conversion efficiency is close to one.

PACS. 32.80Pj – Optical cooling of atoms; trapping.
PACS. 42.50Vk – Mechanical effects of light on atoms, molecules, electrons, and ions.

Introduction. – Continuous beams of slow atoms are of interest for many applications in atomic spectroscopy, collision studies, atom optics, atom interferometry, and atomic frequency standards. Cold atomic beams have been produced from thermal beams using various techniques including slowing of thermal beams by frequency-chirped lasers [1], [2] or by Zeeman tuning [3]. Magneto-optical compression has been used in combination with velocity-selective atomic-beam deflection [4] or moving molasses loaded from a slowed thermal beam [5], [6] to increase atomic density. Isotropic cooling has also been applied to reduce the average velocity of thermal atomic beams [7], [8]. More recently, a simplified scheme based on a 3D magneto-optical trap (MOT) loaded from a vapour has demonstrated its ability to produce a beam of cold rubidium atoms by unbalanced light pressure [9].

A 2D MOT has definite advantages as a continuous source of cold atoms since trapping is restricted to two dimensions and only damping forces must be overcome to extract atoms along the third direction. Trapping efficiency of a 2D trap is as high as one half that of a 3D trap [10]. Several extraction mechanisms have been proposed [11]. Recently, continuous beams of cold atoms extracted from a 2D MOT with a magnetic field or with a moving molasses were demonstrated [12].

(*) Present address: Federal Office of Metrology, CH-3084 Wabern, Switzerland.
(**) Present address: Laboratoire de Probabilité, Université Pierre et Marie Curie, Paris, France.

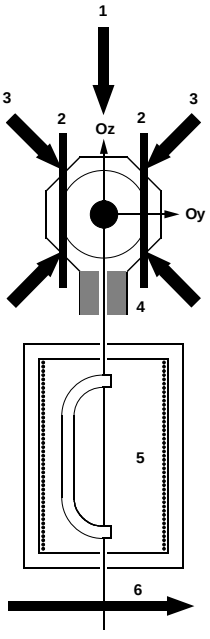

Fig. 1

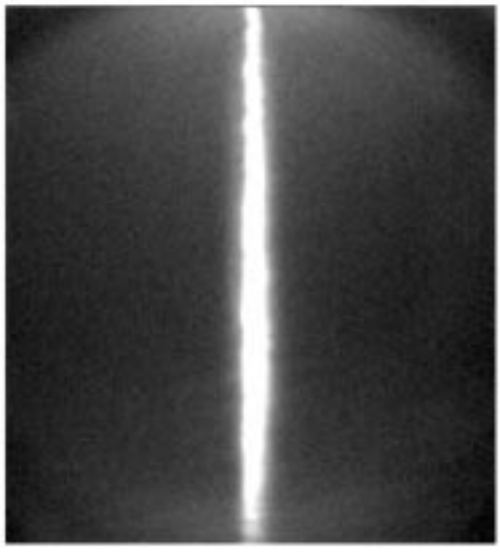

Fig. 2

Fig. 1. – Continuous-beam cesium resonator. 1: static magnetic field; 2: 2D magnetic gradient; 3: cooling beams (Ox beams not shown); 4: cesium getter; 5: Ramsey cavity; 6: probe beam.

Fig. 2. – Cold-atoms cloud in the anisotropic trap ($L = 30$ mm, $N = 2 \cdot 10^8$ at., $T = 40$ μK).

In this letter, we describe the generation of a continuous beam of very slow (0.7–3 m/s) and very cold ($T \lesssim 200$ μK) cesium atoms from a 2D MOT. The average velocity and the temperature are comparable to the lowest reported to date [5], but were obtained in continuous operation, in a vapor cell. The total flux extracted is close to the trapping rate of our MOT. As in [6], [12], but in contrast to [5], [9], the atomic beam is free from any superimposed laser beam, a clear advantage whenever the cold beam is to be used in precision experiments.

Experimental setup. – Our σ^+-σ^- MOT (fig. 1) uses three retroreflected cooling beams, two of which are in the Oyz-plane at 45° with respect to the vertical direction. The third cooling beam is parallel to the Ox-axis. Each cooling beam has a power of about 20 mW and a diameter at $1/e$ of 18 mm. An additional repumping beam is added to the Ox-beams.

To avoid trapping in the vertical direction we use an anisotropic magnetic gradient produced by opposing currents in four vertical copper wires (up to 0.125 T/m). This MOT configuration combines horizontal trapping (Oxy) with a vertical molasses (Oz). The required compensation fields (Ox, Oy) and extraction field (Oz) are produced by three sets of Helmholtz coils.

Atoms falling from the trap pass through a small microwave resonator (Ramsey cavity). They are detected 390 mm below trap center by fluorescence in a probe beam, which is locked either to the $|F = 4\rangle \rightarrow |F' = 5\rangle$ or to the $|F = 3\rangle \rightarrow |F' = 2\rangle$ transition. Figure 2 shows the anisotropic cloud of cold atoms containing $2 \cdot 10^8$ atoms at 40 μK.

Atomic drift in a magnetic field. – When a homogenous magnetic field B_z is applied, trapped atoms thermalize around a drift velocity $v_\mathrm{d} \neq 0$. This velocity is measured *vs.* B_z by

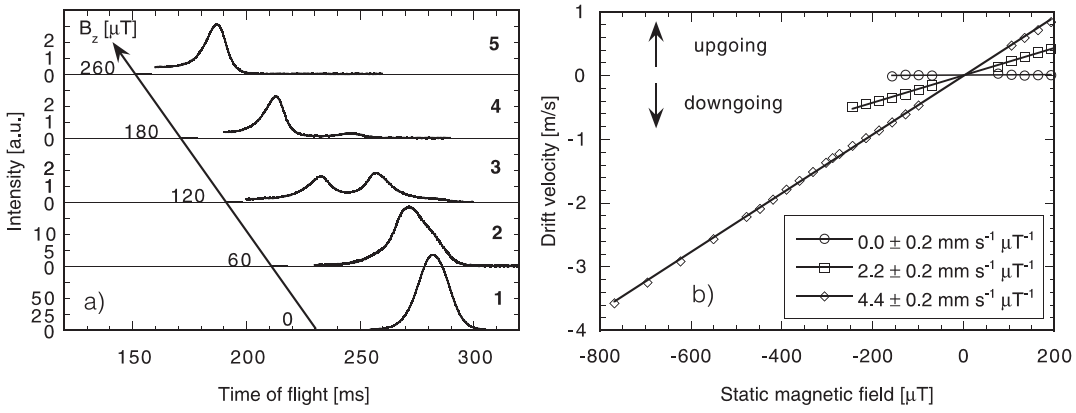

Fig. 3. – a) TOF spectra evolution with magnetic field. b) Drift velocities *vs.* magnetic field.

the TOF technique. Atoms fall in three different velocity classes: a *zero-velocity* class (peaks visible at $t = 282\,\mathrm{ms}$ in curves 1, (2, 3) of fig. 3 a)) and two field-dependent velocity classes (*low-velocity* peak: curves 2, 3 of fig. 3 a); *high-velocity* peak: curves (2), 3–5 of fig. 3 a)) with drift velocities depending linearly on the magnetic field (fig. 3 b)). Moreover the fluorescence signal decreases drastically between 0 and 100 μT (notice vertical scales in fig. 3 a)) as the increasing atomic loss rate reduces the steady-state number of trapped atoms contributing to the TOF signal.

The *zero-velocity* peak is due to atoms that remain trapped in local potential wells associated with the 3D σ^+-σ^- standing waves [11]; it disappears when $|B_z| > 150$ μT.

The *low-velocity* class is characterized by the measured drift coefficient of $2.2\,\mathrm{mm\,s^{-1}\,\mu T^{-1}}$, significantly lower than the $2.98\ \mathrm{mm\,s^{-1}\ \mu T^{-1}}$ predicted [13] and measured [14] for a 1D σ^+-σ^- molasses in a longitudinal magnetic field ($\mathbf{B} \parallel \mathbf{k}$); the discrepancy would be even worse if one simply multiplied the predicted 1D drift velocity by $\sqrt{2}$ to account for our 2D, 45° beam geometry, in which case the theoretical velocity would become $4.22\ \mathrm{mm\ s^{-1}\ \mu T^{-1}}$. It is, however, in good agreement with the theoretical value $2.1\ \mathrm{mm\,s^{-1}\ \mu T^{-1}}$ obtained [15] by a full quantum treatment in a 2D geometry that matches our experiment. Furthermore, Drewsen *et al.* [16] have observed a substantial reduction of the magnetic drift velocity from 1D to 3D molasses. They also note a dependence on the laser detuning. In our experiment, this detuning was kept fixed at -2.5Γ.

The third, *high-velocity* class appears only at relatively high values of magnetic field. The two field-dependent velocity classes only coexist when $100\,\mu\mathrm{T} \leq |B_z| \leq 250$ μT. While the temperature of the *low-velocity* atoms is typically 50 μK, well under the Doppler-limit (127 μK for Cs), TOF spectra show that the temperature of the *high-velocity* atoms increases with magnetic field from 50 μK to 150 μK in the range investigated.

Multiple-peaked velocity distributions have been predicted in a comprehensive study [17] of 1D molasses in a magnetic field. Velocity-selective resonances may appear at $v_\mathrm{d} = \pm\frac{\omega_z}{2k}; \pm\frac{\omega_z}{k}$, where ω_z is the Zeeman frequency in the ground state. In an experiment sensitive to the velocity component parallel to $\mathbf{B}$, however, the only velocity expected is $\frac{\omega_z}{k}$, and indeed opposite drift velocities are not observed simultanously in our experiment (fig. 3 b)). An alternative interpretation of a double-peaked velocity distribution is the transition from sub-Doppler to Doppler cooling mechanisms in an increasing magnetic field, as calculated in [18]-[20] and recently observed [21]. In these 1D models the Doppler to sub-Doppler velocity

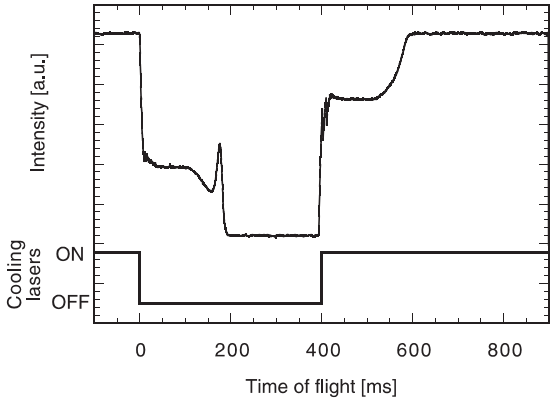

Fig. 4

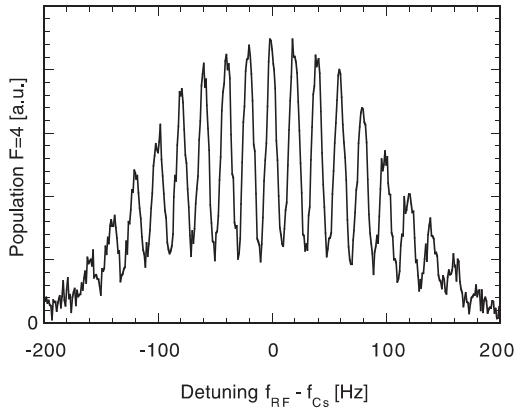

Fig. 5

Fig. 4. – Continuous beam with a homogenous magnetic field. The residual TOF signal occurs after 180 ms and the continuous beam intensity is the DC level difference around 580 ms.

Fig. 5. – Ramsey fringes at the first RF-power. The measured and calculated FWHM are 10 Hz.

ratio is g_e/g_g, the ratio of the excited-state to ground-state Landé factor. This ratio is equal to 1.6 for cesium and should be compared to the 2.0 ± 0.2 measured in our experiment. Calculations in a 2D, 45° geometry are still needed to confirm this interpretation, which is also supported by the observed temperature difference between the two velocity classes.

Continuous beam. – As already mentioned above, the static magnetic field provides a tool for producing a cold-atoms continuous beam. Figure 4 shows the fluorescent intensity transients from atoms crossing the probe beam (upper curve) when the cooling lasers are shut off during 400 ms (lower curve). Ignoring the spurious sharp transients at $t = 0$ and $t = 400$ ms (thermal atoms background), we observe the residual TOF signal 180 ms after light cut. This signal is due to atoms still in the trap when the cooling lasers are shut off. After switching on the cooling lasers again ($t = 400$ ms), it takes the same 180 ms to see a step increase of the fluorescence signal. This increase is evidence of cesium atoms being extracted continuously and reaching the probe beam from that time on. The continuous beam intensity is measured by the difference of DC levels around 580 ms, and coincides with the transition to the single-peak TOF profile where only the fastest atoms contribute.

Ramsey fringes. – We use a Ramsey cavity with a free precession length of 130 mm. As the continuous fluorescence signal is very weak, we modulate the RF-power sinusoidally at 3 Hz and detect synchronously the fluorescence. Figure 5 shows Ramsey fringes produced with our cold-cesium continuous beam at the first optimal RF-power (π-pulse at zero detuning). The measured and calculated FWHM are 10 Hz. Over 200 Hz detuning, the fringe contrast becomes too weak to allow a temperature estimate, because of the Rabi envelope decay.

Calculations show that at small RF detunings (first Rabi lobe), the fringe contrast is strongly dependent on RF power. At high detunings ($\approx$ 300 Hz), however, the fringe contrast is power-independent, but is most sensitive to the width of the velocity distribution. Figure 6 b) shows theoretical Ramsey fringes calculated for a 3π-pulse. The reduction of contrast observed at high detuning for the second optimal RF-power (fig. 6 a)) is used to estimate the axial velocity spread. By fitting the relative fringe contrast of theoretical Ramsey patterns to the

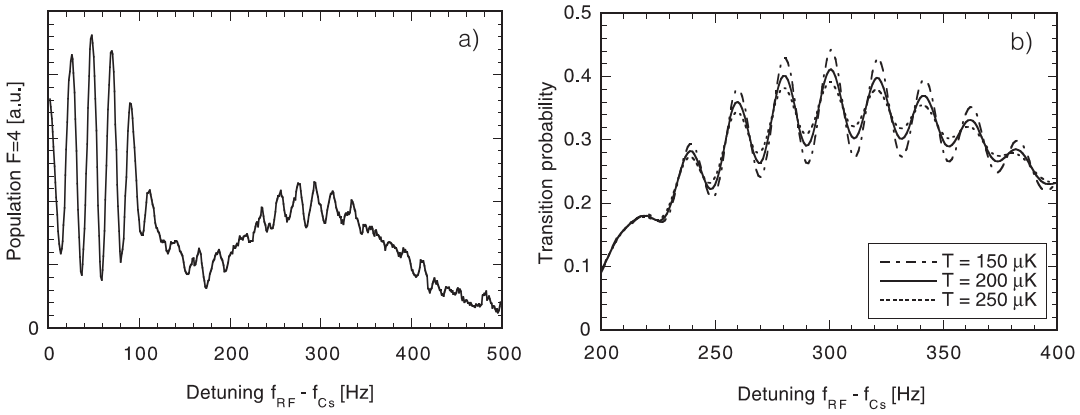

Fig. 6. – a) Smoothed Ramsey fringes for the second optimal RF-power. b) Ramsey fringes calculated for a 3π-pulse and using three different longitudinal velocity distributions.

experimental pattern, we estimate the temperature at $T = 200 \pm 20$ μK. This is an upper bound to the actual temperature since a weak effect of the RF-power modulation on the fringe position has not been taken into account in the fitting procedure.

Beam flux. – The beam flux is measured through the fluorescence intensity in the probe beam, taking into account non-resonant depumping when the probe beam is near saturation intensity. At $B_z = 300$ μT, we obtain a flux density $5 \cdot 10^6$ at. s^{-1} cm^{-2} or $7.6 \cdot 10^9$ at. s^{-1} sr^{-1}. Assuming that the transverse temperature is equal to the axial measured temperature, the total flux is $1.3 \cdot 10^8$ at./s, which is comparable to the capture rate of the trap ($2 \cdot 10^8$ at./s). We conclude that the *trap-to-atomic-beam* conversion efficiency is, within experimental errors, nearly one and that in the present stage, the atomic flux is mostly limited by the power available from the cooling lasers (presently 60 mW). At low field, the beam flux shows a threshold correlated with the appearance of the *high-velocity* class ($B_z \approx 100$ μT). At fields higher than 300 μT, the beam intensity decreases slowly (to one half its maximum value at $B_z \approx 700$ μT). At this level, the vertical field is equal to the trapping field ($70 \cdot 10^{-3}$ T/m) 10 mm away from the trap center and is therefore expected to interfere noticeably with the capture process, preventing atoms from ever reaching the trap center.

Most slow atomic beams produced so far have been obtained in pulsed operation from a thermal beam preslowed by a chirped counterpropagating laser [4], [5], [7]. While the loading rate and resulting flux are high (10^9 to 10^{10} at./s), the technique is not suitable for producing very slow (< 5 m/s) vertical beams. Continuous cold beams differ considerably in flux, velocity and width of the velocity distribution: the atomic beam extracted using intensity imbalance [9] has a flux of $5 \cdot 10^9$ at./s, with a velocity of 14 m/s and a velocity spread of 2.7 m/s; the continuous beam of Weyers *et al.* [12] extracted by a moving molasses has a flux of 10^6 at./s, an average velocity ranging from 2 to 6 m/s and a velocity spread of 0.6 m/s; our flux ($1.3 \cdot 10^8$ at./s) could be increased by using more powerful cooling lasers without affecting the low velocities (0.5–4 m/s) and low velocity spread (0.26 m/s at 1.3 m/s) already achieved.

Conclusion and perspectives. – We have demonstrated a simple and efficient way of producing a very slow beam of cold atoms from a vapour-loaded 2D MOT. The slow beam combines several features (continuous operation, lowest velocity and velocity spread to date, no overlap with a laser beam) that make it ideally suited for high-precision measurements

in spectroscopy, collision studies, atomic interferometry and atomic frequency standards. We have then used this continuous beam to obtain an atomic resonance signal (Ramsey fringes) as an alternative to the pulsed atomic fountain. These first results open the way to the development of a continuous beam frequency standard [22]. Transverse cooling may prove useful to reduce the beam divergence and thus to further increase the beam flux.

This work was supported by the Federal Office of Metrology and by the Swiss National Science Foundation. We thank one of the referees for pointing out the results on magnetic drift in 3D molasses mentioned in [16].

REFERENCES

[1] Ertmer W., Blatt R., Hall J. L. and Zhu M., *Phys. Rev. Lett.*, **54** (1985) 996.

[2] Sheehy B., Shang S. Q., Watts R., Hatamian S. and Metcalf H., *J. Opt. Soc. Am. B*, **6** (1989) 2165.

[3] Prodan J. V., Phillips W. D. and Metcalf H., *Phys. Rev. Lett.*, **49** (1982) 1149.

[4] Nellesen J., Werner J. and Ertmer W., *Opt. Commun.*, **78** (1990) 300.

[5] Riis E., Weiss D. S., Moler K. A. and Chu S., *Phys. Rev. Lett.*, **64** (1990) 1658.

[6] Swanson T. B., Silva N. J., Mayer S. K., Maki J. J. and McIntyre D. H., *J. Opt. Soc. Am. B*, **13** (1996) 1833.

[7] Ketterle W., Martin A., Joffe M. A. and Pritchard D. E., *Phys. Rev. Lett.*, **69** (1992) 2483.

[8] Batelaan H., Padua S., Yang D. H., Xie C., Gupta R. and Metcalf H., *Phys. Rev. A*, **49** (1994) 2780.

[9] Lu Z. T., Corwin K. L., Renn M. J., Anderson M. H., Cornell E. A. and Wieman C. E., *Phys. Rev. Lett.*, **77** (1996) 3331.

[10] Dudle G., Sagna N., Thomann P., Aucouturier E., Petit P. and Dimarcq N., in *Proceedings of the Fifth Symposium on Frequency Standards and Metrology, 15-19 October 1995, Woods Hole, MA, USA*, edited by J. Bergquist (World Scientific, Singapore) 1996, p. 121.

[11] Dudle G., Sagna N., Berthoud P. and Thomann P., *J. Phys. B*, **29** (1996) 4659.

[12] Weyers S., Aucouturier E., Valentin C. and Dimarcq N., *Opt. Commun.*, **143** (1997) 30.

[13] Nienhuis G., van der Straten P. and Shang S.-Q., *Phys. Rev. A*, **44** (1991) 462.

[14] Valentin C., Gagné M.-C., Yu J. and Pillet P., *Europhys. Lett.*, **17** (1992) 133.

[15] Castin Y., unpublished.

[16] Drewsen M., Laurent Ph., Nadir A., Santarelli G., Clairon A., Castin Y., Grison D. and Salomon C., *Appl. Phys. B*, **59** (1994) 283.

[17] van der Straten P., Shang S. Q., Sheehy B. and Metcalf H., *Phys. Rev. A*, **47** (1993) 4160.

[18] Walhout M., Dalibard J., Rolston S. L. and Phillips W. D., *J. Opt. Soc. Am. B*, **9** (1992) 1997.

[19] Werner J., Wallis H. and Ertmer W., *Opt. Commun.*, **94** (1992) 525.

[20] Sagna N., Phd Thesis, Université de Neuchâtel (Neuchâtel, Switzerland) 1996.

[21] Walhout M., Sterr U. and Rolston S. L., *Phys. Rev. A*, **54** (1996) 2275.

[22] Berthoud P., Dudle G., Sagna N. and Thomann P., in *Proceedings of the 11th European Frequency and Time Forum, 4-6 March 1997, Neuchâtel, Switzerland*, (Fondation Suisse Recherche Microtechnique, Neuchâtel, Switzerland) 1997.